Phonon transport in nanowires coated with an amorphous material: An atomistic Green's function approach

N. Mingo and Liu Yang
Eloret Corporation, Mail Stop N229-1, NASA-Ames Research Center, Moffett Field, California 94035-1000, USA

(Received 31 October 2002; revised manuscript received 10 September 2003; published 11 December 2003)

An approach is presented for the atomistic study of phonon transport in real dielectric nanowires via Green's functions. The formalism is applied to investigate the phonon flow through nanowires coated by an amorphous material. Examples for a simple model system and for real Si nanowires coated by silica are given. New physical results emerge for these systems, regarding the character of the transition from ballistic to diffusive transport, the low-temperature thermal conductance, and the influence of the wire-coating interface on the thermal transport. An efficient treatment of phonon scattering by the amorphous coating is also developed, representing a valuable tool for the investigation of thermal conduction through amorphous-coated nanowires.

DOI: 10.1103/PhysRevB.68.245406 PACS number(s): 63.22.+m, 66.70.+f, 68.65.La

I. INTRODUCTION

The problem of phonon transport through dielectric wires of nanometer thickness[1] is of special interest at present, since accurate measurements of thermal conduction in these systems begin to be available.[2–4] Theoretically, this problem has been considered by different approaches. Some of these are the Boltzmann transport equation (BTE),[5] Molecular dynamics (MD),[6,7] and the transmission function approach.[8–13] The BTE has been succesfully used in nanowire transport at high temperatures, for systems where the resistive length of the wire is long enough for the transport to be diffusive. Molecular dynamics has the advantage that it can accurately consider the anharmonic interactions between the atoms. MD was applied to nanowires in Ref. 6, for example. It is nonetheless difficult to study low temperatures using MD, since it provides a classical description of the system.

The transmission function approach is very well suited to study cases when phonons flow ballistically or semiballistically. In the limit of very low temperatures, an elastic continuum model provides a good description of the phonon flow. This model has yielded new insight into the problem of phonon scattering by surface roughness, for example, where the transition from ballistic to diffusive transport[8] and the low-temperature ''dip'' in the quantized thermal conductance[11] have been investigated. Transmission function approaches have also been successfully applied to study the heat flow through a mesoscopic link,[14] a nanocrystal,[15] and monatomic chains.[9] Despite these excellent works, and unlike the case of electron transport, the use of the transmission function approach in phonon transport is still scarce.

In this paper we develop a transmission function approach, and apply it to study a problem that has not been theoretically investigated before: the phonon transport along nanowires in which part of the length is surrounded by a thick coating of amorphous material. This is an important problem, since most dielectric nanowires are naturally coated by a layer of amorphous material.[1,16]

After explaining the general formalism, its use is illustrated by the study of phonon transmission through two concrete systems: a 1D (one-dimensional) chain partially coated with an amorphous layer and real 3D nanowires with part of their length coated by a silica layer. Three main phenomena are investigated.

(a) *The transition from ballistic to diffussive transport*. Explicit curves of how this transition takes place are shown, as a function of frequency and coated length.

(b) *The low-temperature conductance*. It is found that a phenomenon similar to the dip occurring in rough-edge uncoated wires,[11] occurs also in amorphous-coated wires, although displaying some differences with respect to the former case.

(c) *The effect of the wire-coating interface*. We find an interesting saturation effect as a function of the coupling strength between the atoms at the interface. We also show the important influence of the interatomic link number and configuration on the phonon transmission.

Our approach is different from other studies in many respects, given as follows.

(1) An atomistic description is used. This is necessary since we are interested in how the atomic structure of the interface between the wire and the coating affects transport. This also enables to consider the whole dispersive spectrum, and not only the lower frequencies. Although excellent atomistic investigation of transport through monatomic chains was done in Ref. 9, we have not been able to find any other transmission function atomistic study of larger systems, such as the Si nanowires considered here. Despite the method is similar to that of tight-binding electron transport, it is important to provide a complete and independent derivation of the formulas in the phonon framework, specially for those readers not familiar with the theory of electron transport. Part of the paper is devoted to do this in detail.

(2) We present a method that allows us to treat the amorphous overlayer in an efficient manner. As we will see, the presence of the amorphous overlayer introduces a problem of overwhelming computational demand. We develop a technique that is able to yield the thermal conductance in the limit of thick overlayer, with much less computational effort. The validity of this approach is explicitly shown with one example.

The structure of the paper is as follows. Section II explains the formalism. An introduction to the transmission function concept (Sec. II A) is followed by the core of the

method, Sec. II B, where we derive the formulas to compute the phonon transmission function. Afterwards, Sec. II C describes the specific self-consistent technique that enables us to treat the amorphous coating surrounding the wires. Section III shows results for the two examples treated. Conclusions are summarized in Sec. IV.

II. METHOD

A. The transmission function in thermal conductivity and conductance

Both the thermal conductivity and the thermal conductance can be obtained by the same single approach. Let us imagine a perfectly harmonic and translationally invariant nanowire, totally free of defects. The wire is free standing, so that there is no heat leakage from the boundary. The harmonicity assumption implies that, unless there is scattering due to disordered defects or impurities, the thermal conductance of the whole wire would be independent of its length. In this situation, the heat flux associated with a small temperature difference ΔT between the two wire ends is given by the sum of the contributions of the individual phononic subbands:[10]

$$J_Q=\sum_\alpha \int_0^{\pi/a}\Delta T\frac{\partial}{\partial T}\left[\frac{1}{e^{\hbar\omega_\alpha(k)/k_BT}-1}\right]\frac{\partial\omega_\alpha}{\partial k}\hbar\omega_\alpha(k)\frac{dk}{2\pi}$$

$$=\Delta T\sum_\alpha \int_{\omega_\alpha^{init}}^{\omega_\alpha^{fin}}\frac{\partial}{\partial T}\left[\frac{1}{e^{\hbar\omega_\alpha(k)/k_BT}-1}\right]\hbar\omega\frac{d\omega}{2\pi},$$

where α labels the phonon subbands, a is the wire's unit-cell length, k_B is Boltzmann's constant, k is the wave vector in the axial direction, $\omega_\alpha(k)$ is the dispersion relation of subband α, $\omega_\alpha^{init(fin)}$ is the lower- (upper-) frequency limit of the subband, and ω is the frequency. We note that the phonons inside the wire have a nonequilibrium distribution different from the Bose-Einstein type. As it is clear from the second line, it is not necessary to know the dependence of ω_α on k, but only the frequency limits of the subband.

The (length independent) thermal conductance for this limit is then

$$\sigma_{sat}=\sum_\alpha \int_{\omega_\alpha^{init}}^{\omega_\alpha^{fin}}\frac{\partial}{\partial T}\left[\frac{1}{e^{\hbar\omega/k_BT}-1}\right]\hbar\omega\frac{d\omega}{2\pi}. \tag{1}$$

In general, however, one has a nanowire with disordered scattering sources along a finite length. In such a case we no longer have translational periodicity, and we cannot define anything like a ''phonon band dispersion.'' Nevertheless, the concept of transmission channels is still valid. As it was shown by Landauer,[17] no matter how scatterers are distributed in the system, one can always calculate a transmission function $\Xi(\omega)$, which describes the propagation of quasiparticles between two reservoirs connected to the system, with different chemical potentials. In contrast to translationally periodic systems, where the conduction channels always yield integer quanta of transmission, now the waves can be partially reflected resulting in nonintegral transmissions. Thus in this case, instead of Eq. (1), we have

$$\sigma=\int_0^{\omega^{fin}}\Xi(\omega)\frac{\partial}{\partial T}\left[\frac{1}{e^{\hbar\omega/k_BT}-1}\right]\hbar\omega\frac{d\omega}{2\pi}, \tag{2}$$

where the phonon spectrum extends between frequencies 0 and ω^{fin}. Equation (2) is of general validity and involves no approximations. (This equation is rigorously derived in Sec. II B 3.) In the following section we explain how Ξ is calculated exactly for independent phonons.

Scattering causes the conductance to vary with the nanowire's length. For 3D systems in the diffusive regime, the conductance varies inversely proportional to the system's length L. Because of this one usually defines a ''conductivity,'' as

$$\kappa=\frac{L\sigma(L)}{s}, \tag{3}$$

where s is the sample's cross section. However, for nanowires, the length dependence of σ cannot be just assumed to have a $1/L$ form, but needs to be calculated. For short L, σ saturates to σ_{sat}. For long L the behavior depends on the type of scattering and the wire properties. The transition between the two limits also constitutes an important problem (studied in Sec. III). In order to attack these issues, the transmission function has to be calculated for the atomically described, nonperiodical, infinite system. The formalism allowing to do this is explained in the following section.

B. Calculation of the transmission function

1. Interatomic potentials and the dynamical matrix

The system's motion is determined by its dynamical matrix, obtained from the interatomic potentials of the system.[18] The nondiagonal elements of the dynamical matrix **K** are calculated as

$$k_{ij}=\frac{\partial^2 E}{\partial u_i\partial u_j}, \tag{4}$$

where E is the energy and u_i is the displacement of the ith degree of freedom with respect to its equilibrium value. The diagonal elements are $k_{ii}=\Sigma_{j\neq i}-k_{ij}$.[19]

The dynamical equation of the system is

$$(\omega^2\mathbf{M}+\mathbf{K})\overline{u}=\overline{0}, \tag{5}$$

where **M** is a diagonal matrix with elements corresponding to the masses of the constituent atoms, and ω is the vibrational frequency. This problem is analogous to that posed by a nonorthogonal Hamiltonian in the case of electrons, if we replace the energy, Hamiltonian, and overlap, by the square frequency, dynamical matrix, and mass matrix, respectively.[20,21]

The presence of matrix M instead of the identity matrix introduces mathematical difficulties, if Green's functions are used. The issue has been elegantly dealt with in the theory of nonorthogonal tight binding:[21] the ''nonorthogonal'' problem is equivalent to the ''orthogonal'' one

$$(\omega^2\mathbf{I}+\mathbf{M}^{-1/2}\mathbf{K}\mathbf{M}^{-1/2})\overline{u}=\overline{0}. \tag{6}$$

The elements of the ''orthogonalized'' dynamical matrix elements are explicitly defined as

$$\tilde{k}_{ij} = -\frac{k_{ij}}{\sqrt{M_i M_j}}, \tag{7}$$

and the dynamic equation is recast as

$$(\omega^2 \mathbf{I} - \tilde{\mathbf{K}})\bar{u} = \bar{0}, \tag{8}$$

which now can be treated using Green's function methods.

2. Local heat current density

We are faced with the problem of calculating the local heat flow. The following paragraphs derive the necessary equations. The section following this one will express all the equations in terms of Green's functions, so that there is no need to calculate individual wave functions.

Let us consider an arbitrary wave (not necessarily an eigensolution) $u_i(t)$, propagating in the system. The total energy can be expressed as a sum over each degree of freedom, $E = \Sigma_i E_i$, with

$$E_i = -\frac{1}{2}\sum_j u_i k_{ij} u_j + \frac{M_i}{2}\dot{u}_i^2. \tag{9}$$

Using $M_i \ddot{u}_i = -k_{ij} u_j$, the local change of energy with time is

$$\frac{dE_i}{dt} = \frac{1}{2}\sum_j (\dot{u}_i k_{ij} u_j - u_i k_{ij} \dot{u}_j) \equiv \sum_j J_{ij}. \tag{10}$$

The local current between each pair of local degrees of freedom is thus naturally defined as

$$J_{ij} = \tfrac{1}{2}(\dot{u}_i k_{ij} u_j - u_i k_{ij} \dot{u}_j). \tag{11}$$

For a given phonon of frequency ω we rewrite u and $\dot{u}$ in terms of the complex wave $\phi(t) \equiv \psi e^{i\omega t}$:

$$u_i(t) = \mathrm{Re}[\phi_i(t)]/\sqrt{M_i} \equiv \phi_i^R(t)/\sqrt{M_i}, \tag{12}$$

$$\dot{u}_i(t) = -\omega \mathrm{Im}[\phi_i(t)]/\sqrt{M_i} \equiv -\omega \phi_i^I(t)/\sqrt{M_i}. \tag{13}$$

Hence, the current associated with that particular phonon between the i and j local degrees of freedom is

$$J_{ij} = \tfrac{1}{2}\omega(\phi_i^R \tilde{k}_{ij} \phi_j^I - \phi_i^I \tilde{k}_{ij} \phi_j^R) = \frac{\omega}{2}\mathrm{Im}(\phi_i^* \tilde{k}_{ij} \phi_j). \tag{14}$$

ϕ are solutions of the eigenvalue problem, Eq. (8). The normalization condition for the phonon amplitude follows from equating the wave's energy to $\hbar\omega$ as

$$\sum_i |\phi_i|^2 = 2\hbar/\omega. \tag{15}$$

3. The total current

We now proceed to derive the expression for the total heat current given exclusively in terms of Green's functions. To this end, we subdivide the whole system into three regions, as indicated in Fig. 1. The two interfaces define four special groups of atoms labeled α, a, b, and β, as depicted in the figure. An atom belongs to one of these groups if there is a nonzero element of the dynamical matrix linking it to another atom on the opposite side of the interface. In what follows, a bar on top of a symbol, say $\bar{\varphi}$, indicates the one column matrix formed by the values of φ_i at each degree of freedom of the particular group of atoms considered. A parenthesis denotes the subsystem: for example, $\bar{\varphi}(a)$ is formed by values of φ at the atoms of subgroup a only, and its dimension is three times the number of atoms in a. Similarly, a bar below the symbol, say $\underline{\varphi}$, denotes a one row matrix. We denote the traveling-wave solutions of the total system by $\bar{\Phi}_n$. The total current in terms of them is then given by [see Eq. (14)]

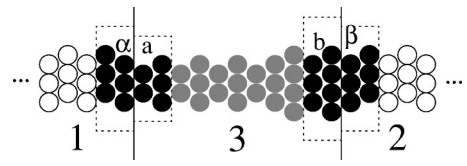

FIG. 1. Nomenclature used in Sec. II B 3. The semi-infinite leads 1 and 2 are projected onto subsets α and β, and the total Green's function for susbsystem 3 only needs to be computed between atoms of subsets a and b.

$$J = \sum_n N_n \frac{\omega_n}{2}\mathrm{Im}[\underline{\Phi}_n^*(b)\tilde{\mathbf{k}}_{b\beta}\bar{\Phi}_n(\beta)], \tag{16}$$

where N_n is the number of phonons in state n.

Using standard scattering theory[20] one can express the eigenfunctions of the total system, Φ_n in terms of the retarded Green's-function matrix of the total system $\mathbf{G}$ and the eigenfunctions of the decoupled system at the left of interface 1 (that is, with the coupling between α and a set to zero). Denoting these wave functions for the decoupled system as $\bar{\phi}(\alpha)$, one has for the waves propagating from α towards β,

$$\bar{\phi}_n(b) = \mathbf{G}_{ba}\tilde{\mathbf{k}}_{a\alpha}\bar{\phi}_n(\alpha), \tag{17}$$

$$\bar{\phi}_n(\beta) = \mathbf{G}_{\beta a}\tilde{\mathbf{k}}_{a\alpha}\bar{\phi}_n(\alpha) = \mathbf{g}_{\beta\beta}\tilde{\mathbf{k}}_{\beta b}\mathbf{G}_{ba}\tilde{\mathbf{k}}_{a\alpha}\bar{\phi}_n(\alpha), \tag{18}$$

where $\mathbf{g}_{\alpha\alpha}$ and $\mathbf{g}_{\beta\beta}$ are the retarded Green's-function matrices corresponding to the decoupled systems (i.e., with $\tilde{\mathbf{k}}_{\alpha a} = \mathbf{0}$ and $\tilde{\mathbf{k}}_{b\beta} = \mathbf{0}$).

Inserting these expressions in the equation for the current we have

$$\begin{aligned} J &= \frac{\mathrm{Im}}{2}\sum_n \Delta N_\omega \omega_n \underline{\phi}_n^*(\alpha)\tilde{\mathbf{k}}_{\alpha a}\mathbf{G}_{ab}^*\tilde{\mathbf{k}}_{b\beta}\mathbf{g}_{\beta\beta}\tilde{\mathbf{k}}_{\beta b}\mathbf{G}_{ba}\tilde{\mathbf{k}}_{a\alpha}\bar{\phi}_n(\alpha) \\ &= \frac{1}{2}\sum_n \Delta N_\omega \omega_n \\ &\quad \times \mathrm{Tr}[\mathrm{Im}\{\bar{\phi}_n(\alpha)\underline{\phi}_n^*(\alpha)\tilde{\mathbf{k}}_{\alpha a}\mathbf{G}_{ab}^*\tilde{\mathbf{k}}_{b\beta}\mathbf{g}_{\beta\beta}\tilde{\mathbf{k}}_{\beta b}\mathbf{G}_{ba}\tilde{\mathbf{k}}_{a\alpha}\}], \end{aligned} \tag{19}$$

where the sum extends to all states of the uncoupled subsystem 1, and

$$\Delta N \equiv N^+ - N^- = \frac{\hbar\omega}{k_B T^2} \frac{e^{\hbar\omega/k_B T}}{(e^{\hbar\omega/k_B T}-1)^2} \Delta T \tag{20}$$

is the occupation difference between phonons traveling forwards and backwards.

It is not feasible to explicitly compute the eigenfunctions $\overline{\phi_n}$ for a semi-infinite system. This can be avoided by expressing everything in terms of Green's functions, which allow to project semi-infinite systems on the atomic groups considered. From the normalization condition, Eq. (15), and the well-known relation between Green's function and the density of states,[19] it follows that, at any infinitesimal frequency square interval, $\{\epsilon, \epsilon + d\epsilon\}$,

$$\sum_{n(\omega_n^2 \in \{\epsilon, \epsilon+d\epsilon\})} \omega_n \overline{\phi}_n(\alpha) \underline{\phi_n^*}(\alpha) = 2\frac{\hbar}{\pi} \mathrm{Im}[\mathbf{g}_{\alpha\alpha}(\epsilon)] d\epsilon, \tag{21}$$

where $\epsilon \equiv \omega^2$. Using this relation, the expression for the current, Eq. (19), becomes

$$J = \int_0^\infty \frac{\hbar\omega}{2\pi} \Delta N(\omega) \Xi(\omega) d\omega, \tag{22}$$

$$\Xi(\omega) = 4\mathrm{Tr}[\tilde{\mathbf{k}}_{a\alpha} \mathrm{Im}[\mathbf{g}_{\alpha\alpha}] \tilde{\mathbf{k}}_{\alpha a} \mathbf{G}_{ab}^* \tilde{\mathbf{k}}_{b\beta} \mathrm{Im}[\mathbf{g}_{\beta\beta}] \tilde{\mathbf{k}}_{\beta b} \mathbf{G}_{ba}], \tag{23}$$

where the transmission function $\Xi(\omega)$ has been defined. The thermal conductance, Eq. (2), follows straightforwardly from Eq. (22). Now we only need to compute Green's functions **g** and **G**, and then use Eqs. (23) and (22) to calculate thermal currents.

4. Calculation of Green's functions for infinite systems without translational periodicity

The system we are treating is infinitely extended in the heat propagation direction, but it does not have translational symmetry. Therefore, the calculation of Green's functions requires the use of projection techniques. The most efficient way to obtain the Green's function of the semi-infinite systems 1 and 2 projected at subsystems α and β is to use the decimation technique,[22] which is based on a renormalization procedure. After $\mathbf{g}_{\alpha\alpha}$ and $\mathbf{g}_{\beta\beta}$ are calculated in this way, one can calculate the total retarded Green's function of the system everywhere in subsystem 3 (Fig. 1) as

$$\mathbf{G}(\omega^2) = [\omega^2 \mathbf{I} - \tilde{\mathbf{k}} - \mathbf{\Sigma}_1(\omega^2) - \mathbf{\Sigma}_2(\omega^2)]^{-1}, \tag{24}$$

where the self-energy matrix $\mathbf{\Sigma}_1$ is defined as $\tilde{\mathbf{k}}_{\alpha a} \mathbf{g}_{aa} \tilde{\mathbf{k}}_{a\alpha}$ on the elements belonging to subset *a*, and zero otherwise, and $\mathbf{\Sigma}_2$ is defined similarly on subset *b*.

C. Self-consistent flux model for efficient computation of boundary scattering

If we know the dynamical matrix, the formalism explained in the previous paragraphs is capable of accounting for any type of scattering mechanism other than anharmonicity (for the role played by anharmonicity, see the Appendix). It is straightforward to include isotopes by varying the mass of given atoms; substitutional impurities may be introduced by varying both the mass of selected atoms and the links to their neighbors; vacancies would be included by removing single atoms and allowing the system to relax; etc. We might thus be tempted to treat boundary scattering in this same spirit, by including surface adsorbates or imperfections that can lead to effective boundary scattering in the nanowire. Adding single adsorbed impurities is a rather simple matter, but could one consider an amorphous overlayer on the same footing? For example, it is known that Si nanowires are covered by an amorphous SiO_2 overlayer, several nanometers in thickness,[1] and it is important to know how this overlayer affects the phonon scattering. A brute force approach would be to input the atomic positions of all constituents in the silica overlayer, as well as the wire, and then calculate the dynamical matrix of the whole system and compute its transmission.

This procedure, however, is a nearly impossible task in practice. The added overlayer considerably increases the size of the system, and it also results in an extremely irregular transmission function, which has to be computed at a very large number of different frequencies. The integration of such a transmission in Eq. (2), consequently, becomes cumbersome. To solve these difficulties, we have developed the self-consistent (SC) flux model. This model's basic idea consists in taking the limit of an infinitely thick overlayer. In the same spirit of the Bethe lattice approach, as used for amorphous materials,[19] we consider the nanowire connected to Bethe lattice branches of the amorphous material (see Fig. 2). The phonon mean free path in amorphous materials is of the order of the interatomic spacing.[23] Therefore, the lack of connectivity in the Bethe lattice approach does not represent a problem. The adequacy of the Bethe lattice approach for the study of amorphous systems has been investigated in Refs. 24 and 25.

When the overlayer is substituted by an infinitely thick one, an essential difference appears. Now the self-energies associated with the overlayer do not correspond to clusters. Therefore, they are no longer purely real, but contain a finite continuous imaginary part. In other words, if one calculates the transmission of the system by Eq. (23), part of the phonon flux will be effectively lost through the side branches, since now they are infinite and allow for the current to go away without returning. However, this is not physically correct, for we know that the overlayer is finite and the heat current must eventually come back to the wire and escape through the contacts. In a steady state, this means that we must allow for an equivalent amount of phonon flux to reenter the system through each of the side branches. One may find a self-consistent solution to this problem in the form of an iterative procedure. This is indeed not necessary, for the self-consistent solution can be directly found by an algebraic method, as we show below.

To clarify the nomenclature in the following discussion, a general scheme of the nanowire with part of its length coated is shown in Fig. 2, left. The represented nanowire is three dimensional, thus each black dot in the figure stands for a

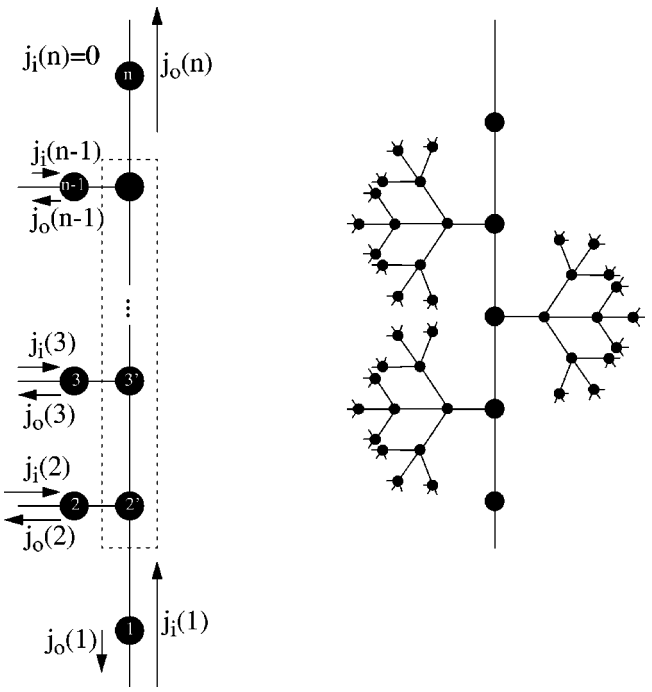

FIG. 2. Left: scheme of a linear chain system showing the nomenclature used in the self consistent flux technique of Sec. II C. Right: scheme of 1D wire with Bethe lattices of coordination 4 attached.

group of atoms, and each line joining dots stands for a set of interatomic links. The dotted line encloses the wire's groups of atoms that are coated. Bethe lattices are attached to those groups of atoms, as shown in the figure. Phonons enter the system through group 1 and exit at the other lead through group n. First of all, we obtain the partial transmissivities $\mathcal{T}$ between every pair of branches in the system, using Eq. (23),

$$\mathcal{T}_{ij}=\frac{4}{N}\mathrm{Tr}[\tilde{\mathbf{k}}_{ii'}\mathrm{Im}[\mathbf{g}_{i'i'}]\tilde{\mathbf{k}}_{i'i}\mathbf{G}_{ij}^{*}\tilde{\mathbf{k}}_{jj'}\mathrm{Im}[\mathbf{g}_{j'j'}]\tilde{\mathbf{k}}_{j'j}\mathbf{G}_{ji}], \tag{25}$$

where i and i' label neighboring atomic subsets belonging to the branch and wire, respectively, for the first branch of the pair, and equivalently j and j' for the second branch. N is the number of degrees of freedom in node i' or j'. (All nodes are assumed to contain the same number of atoms for simplicity.)

We recall that each link to a branch in Fig. 2 may comprise interactions with several atoms, in the three geometrical directions, so Green's functions above are matrices. The transmissivity from one branch to itself is not defined by the above formula. Instead, we must define it as the reflectivity

$$\mathcal{T}_{ii}=1-\sum_{j\neq i}\mathcal{T}_{ij}. \tag{26}$$

We define the "injected" and "outflowing" flux arrays, $\overline{j_i}$ and $\overline{j_o}$ as the fluxes coming "into" and "out of" the system via its surrounding nodes (see Fig. 2). The total flux array $\overline{j}$ is then

$$\overline{j}=\overline{j_i}-\overline{j_o} \tag{27}$$

and it must fulfill

$$j(1)=j_i(1)-j_o(1)=j_o(n) \tag{28}$$

because all the flux coming in through node 1 must finally exit through node n. Also, there is no flux injection from node n, so

$$j_i(n)=0. \tag{29}$$

All the other modes must fulfill

$$j(l)=j_i(l)-j_o(l)=0, \quad \forall\, l\neq 1,n. \tag{30}$$

We can express Eqs. (28)–(30) in matrix form as

$$j_i=\mathbf{A}j_o, \tag{31}$$

with

$$\mathbf{A}=\begin{Bmatrix}1&0&0&\cdots&0&1\\0&1&0&\cdots&0&0\\0&0&1&\cdots&0&0\\\vdots&\vdots&\vdots&\ddots&\vdots&\vdots\\0&0&0&\cdots&1&0\\0&0&0&\cdots&0&0\end{Bmatrix}. \tag{32}$$

On the other hand, the outflowing currents are related to the injected ones by

$$\overline{j_o}=\boldsymbol{\mathcal{T}}\overline{j_i}, \tag{33}$$

which implies

$$\overline{j_o}=\boldsymbol{\mathcal{T}}\mathbf{A}\overline{j_o}. \tag{34}$$

Therefore, the self-consistent array $\overline{j_o}$ is proportional to the eigenvector $\overline{v_1}$ of $\boldsymbol{\mathcal{T}}A$ with eigenvalue 1, such that $\boldsymbol{\mathcal{T}}A\overline{v_1}=\overline{v_1}$. The existence of eigenvalue 1 is guaranteed by the way we have defined $\mathcal{T}_{ii}$ [Eq. (26)] and by the fact that columns 1 and n in matrix $\boldsymbol{\mathcal{T}}A$ coincide.

The transmission corresponds to the outgoing flux at node n when there is one unit of incident flux per degree of freedom in node 1. Thus, imposing $j_i(1)\equiv N=j_o(1)+j_o(n)$, where the second equality follows from Eq. (28) gives

$$\overline{j_o}=\frac{N}{v_1(1)+v_1(n)}\overline{v_1} \tag{35}$$

and the self-consistent transmission is

$$\Xi=j_o(n)=N\frac{v_1(n)}{v_1(1)+v_1(n)}. \tag{36}$$

It can be easily verified that for the uncoated case the calculation using Eq. (36) coincides with that of Eq. (23).

In the following section we explicitly demonstrate that the SC flux approach yields the same result that the calculation using large clusters attached to the wire. Therefore, the SC

flux technique is of tremendous importance, since it enables to study the otherwise untractable problem of thermal transport through thick-amorphous-coated real wires.

III. RESULTS

New physics regarding how the amorphous coating influences the thermal transport through a wire can now be learned using the above method: Does the coating affect all frequencies equally or are there important differences in the scattering as a function of frequency? Does diffusive transport arise? And, if so, how long a segment has to be coated in order for transport to diffusive rather than ballistic? How does transport depend on the coupling at the wire-coating interface? etc.

In the following two sections we present results for two different systems. First, a one-dimensional model, which is simple enough to allow for a thorough investigation without encountering size limitations, and at the same time displays many general features that apply to real systems. Afterwards, we present results for real 3D silicon nanowires.

A. Study of a one-dimensional model

A wide range of interesting phenomena is obtained already in the case where there is only one degree of freedom per atom, in a linear chain. Bethe lattices with also one degree of freedom per atom are attached to a section of the chain. The wire's properties are determined by the value of a spring constant K_W. For the Bethe lattices, we assume them to be linear chains (i.e., $Z=2$ in the nomenclature of Ref. 20), and they are characterized by their spring constant K_B. The third constant involved is the coating-wire interaction K_{BW} connecting the end of the Bethe lattice to the wire.

1. Comparison between SC flux and cluster calculations

First of all, we provide a particular example that demonstrates the equivalence between the SC flux calculation, and the much more computationally demanding calculation using large finite clusters for the coating. The transmission was computed for a system with ten clusters attached to it at ten consecutive atoms. Each of the clusters is composed of 60 overlayer atoms. The transmission, calculated via Eq. (23), is shown in Fig. 3(a). We shall refer to this curve as the ''cluster transmission.'' A large number of closely spaced antiresonances occurs, due to the finite size of the clusters. Thus, the curve had to be computed at many different frequency points.[26]

The transmission given by the SC flux method is shown as the thicker line in Fig. 3(b). We shall refer to it as the ''SC flux transmission.'' Its smooth shape has little visual resemblance with the cluster transmission.

We can now compute the thermal conductance as a function of temperature, using both the cluster and SC flux transmissions, and compare the results. We define the dimensionless thermal conductance as

$$\tilde{\sigma}=\frac{6}{\pi}\frac{\sigma}{k_b\omega_D}, \tag{37}$$

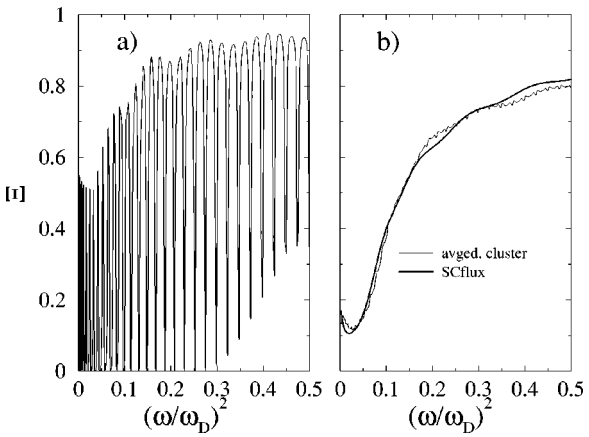

FIG. 3. Comparison between the transmission calculated by using finite clusters as scatterers or the SC flux method with infinite Bethe lattices. (a) Cluster transmission. (Ten clusters comprising 60 atoms each are attached to the chain.) (b) Thick line—SC flux transmission; thin line—the curve in (a) averaged in a range of frequencies around each point. As more atoms are added to the clusters, the averaged curve approaches the SC flux result more closely.

where $\omega_D=2K_B$ is the Debye frequency of the infinite 1D atomic chain. Using Eq. (2), the dimensionless conductance can be evaluated in terms of the dimensionless temperature $\tilde{T}\equiv(k_b/\hbar\omega_D)T$ and the dimensionless frequency $\tilde{\omega}\equiv\omega/\omega_D$, as[27]

$$\tilde{\sigma}=\frac{3}{\pi^2}\int_0^1 \Xi(\tilde{\omega})\frac{\tilde{\omega}^2}{\tilde{T}^2}\frac{e^{\tilde{\omega}/\tilde{T}}}{(e^{\tilde{\omega}/\tilde{T}}-1)^2}d\tilde{\omega}. \tag{38}$$

The dimensionless conductance calculated from the cluster transmission is shown as the thick dashed line in Fig. 4, as a function of the dimensionless temperature. Now this curve can be compared with the thermal conductance calcu-

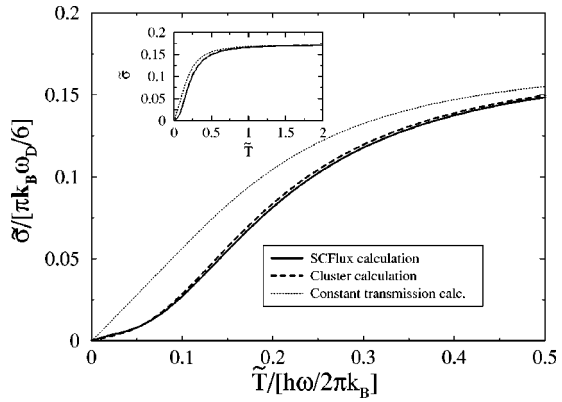

FIG. 4. Comparison between the dimensionless thermal conductance as a function of the dimensionless temperature, calculated from the *cluster* transmission (dashed line) and from the SC flux transmission (solid line). Although the two transmissions have very different shapes (cf. Fig. 3), the conductances obtained from them are nearly the same. The conductance obtained from a *constant* transmission function is also shown (dotted line) to stress the important role played by the frequency dependence of the transmission function.

lated using the SC flux transmission. Remarkably, the latter yields the thick solid curve in Fig. 4; almost exactly the same thermal conductance curve than that computed from the cluster transmission. The reason why the two apparently very different transmissions yield virtually the same conductance can be better understood by averaging the cluster transmission in a range of frequencies, so as to smooth out its structure. We have convolved the curve in Fig. 3(a) with a truncated Gaussian kernel extended $\pm\omega_D/60$ around each point. The cluster transmission averaged in this way is shown as the thin line in Fig. 3(b), and is very close to the SC flux transmission.

Thus we see that the transmission calculated with the SC flux method does indeed yield the same thermal conductance as if we include the thick coating in the form of large finite clusters. But the SC flux method requires a much smaller computation, because it yields a smooth transmission curve, while the cluster calculation needs to evaluate a far larger number of points in order to account for the closely spaced antiresonant structure associated with the finite clusters.

To quantify the difference between the *real* conductance and the one obtained using a *frequency independent* boundary scattering, the latter is also plotted in Fig. 4, as the thin dotted curve. The value of the constant transmission has been fixed to yield the same limiting conductance in the $\omega\to\infty$ limit as the real conductance curves (see inset of Fig. 4). As the figure shows, important differences between the oversimplified constant transmission model and the real transmission calculation exist up to well above the debye temperature.

2. Study of the transmission function

Now we proceed to study the behavior of the transmission as a function of the different physical parameters in play. More concretely, we want to know how the transmission depends on frequency ω, coated length L, and strength of the interface spring constant K_{BW}. The analysis will show us how the system goes from ballistic to diffusive behavior, as a function of these physical parameters.

We set K_W to be the unit of spring strength. The mass of all atoms M is defined also as 1. Frequencies are in units of $\sqrt{K_W/M}$. The coated length L is given in lattice units, being equivalent to the number of Bethe lattices attached.

First let us take a look at the behavior of the transmission function with frequency, in Fig. 5 (for $K_W/K_B=1$ and $K_{BW}=1$). We notice that the effect of boundary scattering is to reduce the transmission rather uniformly throughout the whole frequency range. However, it is apparent that the usual assumption of a constant scattering rate[23,28–30] is only a rough approximation to the real scattering in nanowires. The low-frequency limit behavior displays an important feature: for wires where the coated segment is long enough ($n>3$ in the case shown), the transmission near $\omega\simeq 0$ decreases with increasing frequency. This appears to be the general case, as we will see in the following section. It has a direct physical consequence: the slope of thermal conductance at very low temperatures decreases below its $T=0$ value when temperature increases. This fact has been shown to happen also in the case of surface roughness at noncoated wires[11] (the well-known dip of Ref. 2). We explicitly show this for Si nanowires in the following section.

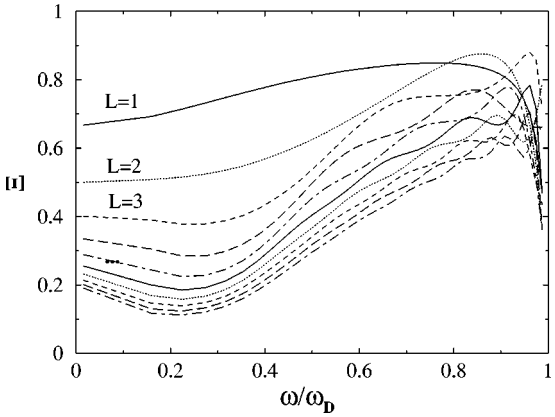

FIG. 5. SC flux transmission as a function of frequency for infinite 1D chain, for coated segments of different lengths L (= number of lattices attached).

In Fig. 5 we have seen that the shape of the transmission function varies as a function of the coated length. Does it attain a limiting shape? And, how is this limit reached? This is the subject of the *diffusive-ballistic transition*. The way it takes place will become clear from the study of the transmission as a function of coated length L. In principle, it is not obvious what type of length dependence one could expect. For pure disorder, for example, an exponential decrease in transmission is obtained in 1D systems due to localization.[31] As another example, for wires with rough edges, an anomalous $L^{-1/2}$ thermal conductance has also been reported under certain conditions.[8] For amorphous-coated wires, the asymptotic behavior turns out to be $\sim L^{-1}$, as we now show.

Analogously to Ref. 32, we write the transmission as

$$\Xi=\Xi_0[1+L/\lambda(L)]^{-1}. \tag{39}$$

This is merely a definition of $\lambda(L)$, and it does not impose any limitations on the form of the transmission. For the present 1D system, the uncoated wire's transmission Ξ_0 is equal to 1 at all frequencies. Now, the form of $\lambda(L)$, plotted in Fig. 6, tells us the length dependence of the transmission. New physical insight can be gained from this figure. First, we see that $\lambda(L)$ quickly tends to an asymptotic value. This means that, for amorphously coated wires, the long L behavior of the transmission follows an L^{-1} dependence.[33] More interestingly, the length it takes $\lambda(L)$ to saturate to its asymptotic value becomes longer as the frequency gets closer to zero. Physically, this implies that the lowest-frequency phonons can still travel nearly ballistically for system lengths at which higher-frequency phonons are transported in an almost totally diffusive fashion. In a practical measurement of nanowire thermal conductivity, this might lead to a wrong estimation of the low-temperature thermal conductivity, if the wire were not long enough.

In the diffusive regime, we can define a frequency dependent relaxation length λ_∞ as the limit

$$\lambda_\infty(\omega)\equiv\lim_{L\to\infty}\lambda(\omega). \tag{40}$$

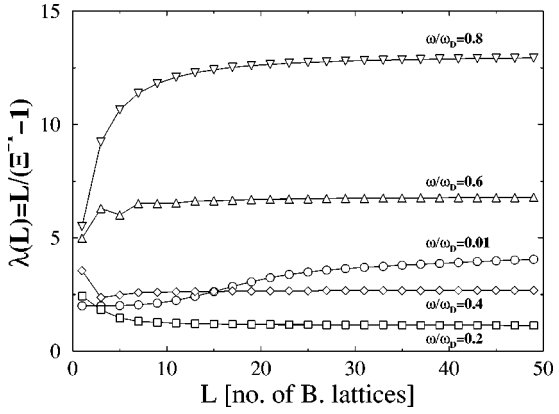

FIG. 6. Plot of $\lambda(L) \equiv (\Xi_0/\Xi - 1)^{-1} L$ as a function of the coated length L, for different frequencies. $\lambda(L)$ asymptotically converges to a limiting relaxation length value $\lambda_\infty(\omega)$ for long enough L.

A very interesting phenomenon arises when we study how this relaxation length depends on the strength of the spring constants coupling the wire to the amorphous coating. We numerically computed λ_∞ at frequency $\omega = 0.05\omega_D$, as a function of the wire-coating coupling strength. The result is plotted in Fig. 7. For decreasing values of the wire-coating coupling K_{BW} the relaxation length quickly increases, as expected. However, if the coupling is made stronger, λ_∞ reaches a minimum and then it increases again as the coupling is increased, approaching an asymptotic value. The existence of this *minimum relaxation length* can be interpreted in microscopic terms: there is an optimum value of the coupling that maximizes the heat-flow exchange to and from the coating, thus maximizing the scattering. For very weak couplings the heat-flow exchange reduction is intuitively obvious. For very strong couplings on the other hand, the linked atoms would behave more like a rigid cluster, thus acting as a hard wall that also confines the phonons to the wire rather than let them enter the amorphous region. From a macroscopic point of view, the relaxation length is minimum when

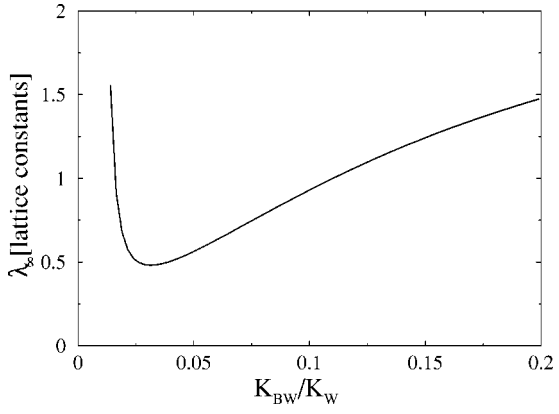

FIG. 7. Phonon relaxation length λ_∞ as a function of the coupling between the wire and its coating lattices. It reaches a minimum and then increases, asymptotically approaching a limiting value. (In the particular case shown here, $\omega = 0.05\omega_D$ and $\lambda \to 2.7$.)

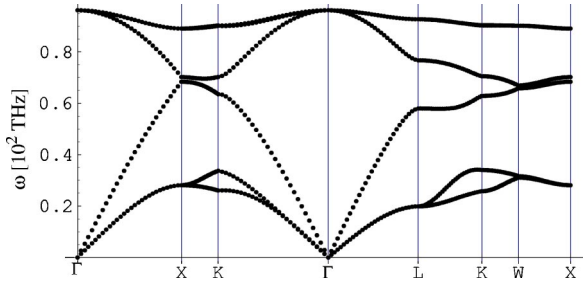

FIG. 8. Phonon dispersion relations calculated for bulk Si using Harrison's potential.

the specularity factor is 0, in the Casimir limit.[34] The minimum of λ_∞ obtained thus translates to this limit, and specularity increases in both ways around this point as a function of K_{BW}.

B. Results for Si nanowires

The advantage of the atomistic description used in this paper is that we can study wires made of ''real'' materials. In other words, we are dealing with the real phonon spectrum of the system: the bands are dispersive and their frequency extension is finite, in contrast with the infinitely extended spectrum in a continuum elastic system.

We proceed to study the transmission of phonons in real Si nanowires, with an amorphous material coating the wire. The phonon dispersion relations of Si are fairly well reproduced with an interatomic potential that includes only two- and three-body terms. We use Harrison's potential.[35] The adequacy of this potential for Si is assessed by the satisfactory dispersion relations calculated with it. We show them for bulk Si in Fig. 8. Despite having only two parameters, the shape and position of the bands are in reasonably good agreement with experimental results.[36,37]

The two-body contribution to the energy is

$$\delta E_0(i,j) = \frac{1}{2} C_0 \frac{(d_{i,j} - d_0)^2}{d_0^2} \tag{41}$$

for every pair of nearest neighbors i and j, where $d_{i,j}$ is the distance between the atoms and d_0 is the lattice equilibrium distance. The three-body contribution is

$$\delta E_1(i,j,k) = \tfrac{1}{2} C_1 \delta\Theta_{i,j,k}^2 \tag{42}$$

for every pair of bonds joining atoms i, j, and k, where $\delta\Theta$ is the deviation with respect to the equilibrium angle between the two bonds in the lattice. Constants $C_0 = 49.1$ eV and $C_1 = 1.07$ eV are taken from Table 9-1 of Ref. 35.

For the coating we again consider Bethe lattices connected to each vibrational coordinate of the boundary atoms. The parameters of the Bethe lattice are chosen to reproduce the frequency range of the known density of states of silica,[38] i.e., 2×10^{14} Hz. A coordination number $Z = 4$ is assumed. We have considered (011) wires of three different widths, shown in Fig. 9. The wires are coated by attaching Bethe lattices only to the outermost atoms. For the 2×2 wire all atoms are at the surface. The 3×3 wire has 16 surface atoms

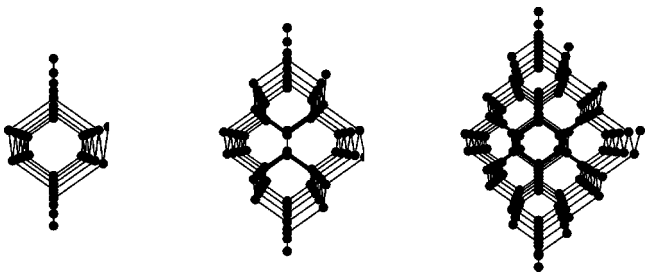

FIG. 9. Cross sections of the three Si nanowires studied: "2×2," "3×3," and "4×4."

and 2 core atoms. The 4×4 wire has 24 surface atoms and 8 core atoms. The phonon dispersion relations for each of them is shown in Fig. 10.

The procedure for the calculation is as follows. First, the nanowire lattice is defined, and the dynamical matrix is obtained for the periodic unit cell, and for the link between two neighboring unit cells. The Bethe lattices are included as a self-energy projected onto their last atom. The self-energy due to the uncoated parts of the wire is calculated in the way of Ref. 22. Then the Green's function of the system is calculated [Eq. (24)]. The partial transmissivity between each pair of branches [Eq. (25)] is then calculated, and the SC flux transmission [Eq. (36)] is computed.

We show how the phonon transmission depends on frequency, for different values of the coated length. Figure 11 shows $\Xi(\omega)$ as the coated length increases from 0 to 5 coated unit cells. In these curves, all three spatial directions of each of the surface atoms are attached to Bethe lattices. The qualitative behavior is an overall uniform decrease of the transmission curve, which maintains the peaks and curve features of the uncoated wire. This is in agreement with the usual assumption of a constant scattering rate. However, quantitatively the boundary scattering rate is not frequency independent, as it is apparent from the relative heights of the peaks at different coating lengths. In the absence of coating, the transmission curve at the lower end of the frequency spectrum has a value of 4. This is always the case, since there are four lowest-frequency branches at all nanowires: one dilatational, one torsional, and two flexural branches.[39] The two flexural branches have a quadratic rather than linear dispersion, as we can see in Fig. 10, being a consequence of the soft character of those modes.

The transmission at the lowest frequency decreases more slowly than that around the first peak (~20 THz), as the coated length becomes larger. Thus scattering is weaker for the lowest-lying modes than for the bulk of transverse modes. This results in a flattening of the transmission as L increases. The narrower the wire, the more pronounced this effect becomes.

The low-frequency behavior of the transmission function also has important physical implications. Similarly as what we saw in the 1D example of Sec. III A, for real Si nanowires the transmission function also decreases below its $\omega=0$ value for small values of the frequency, and increases again as the frequency rises further (see inset in Fig. 12). The result is that, at low, finite temperatures, the thermal conductance divided by T decreases with respect to its zero-

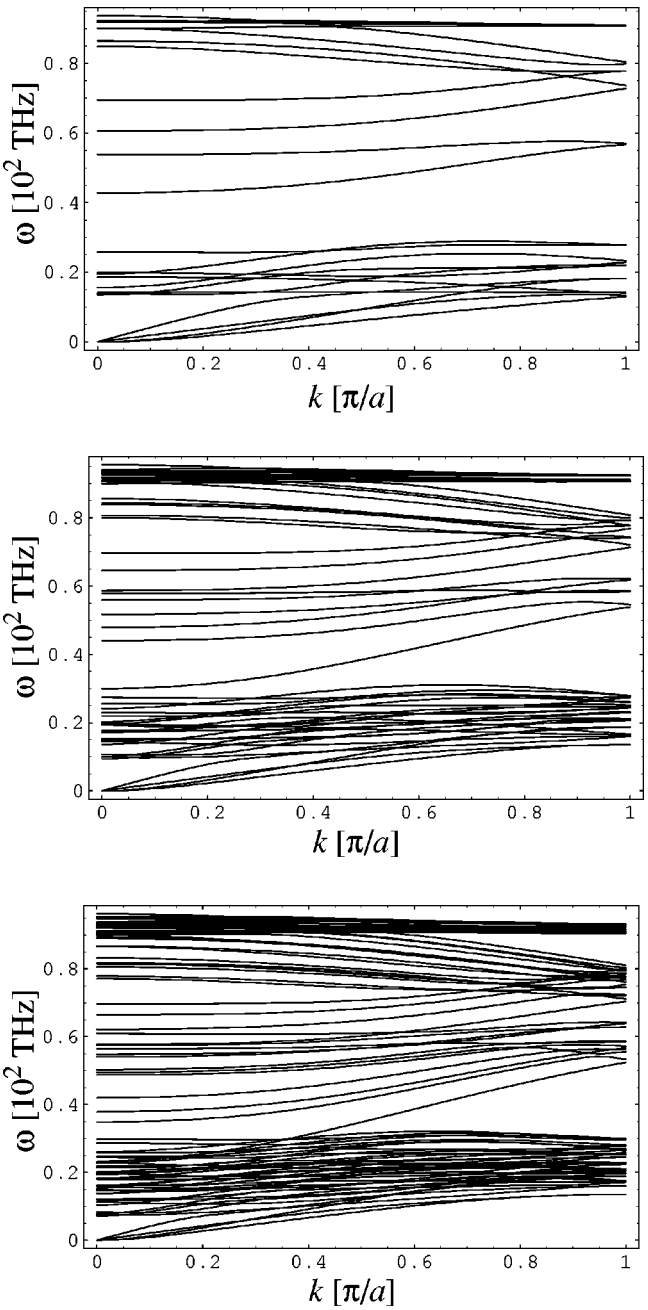

FIG. 10. Phonon dispersion relations for the three Si nanowires in Fig. 9.

temperature value, thus displaying a dip (see Fig. 12). A dip in $\sigma(T)/T$ has been reported in Ref. 2, and theoretically explained in Ref. 11 to be the result of surface roughness scattering. In our case of amorphous-coated nanowires we see that an analogous dip occurs, although the system considered here is basically different from that one, and the conductance reduction phenomenon cannot be considered to be the same one. Some essential differences exist in the case of scattering by amorphous coating with respect to the roughness scattering case. One is that, at zero frequency, the scattering rate is zero in the case of roughness scattering, while it is different than zero in the case of amorphous-coating scattering. As a result, it is possible to measure a conductance

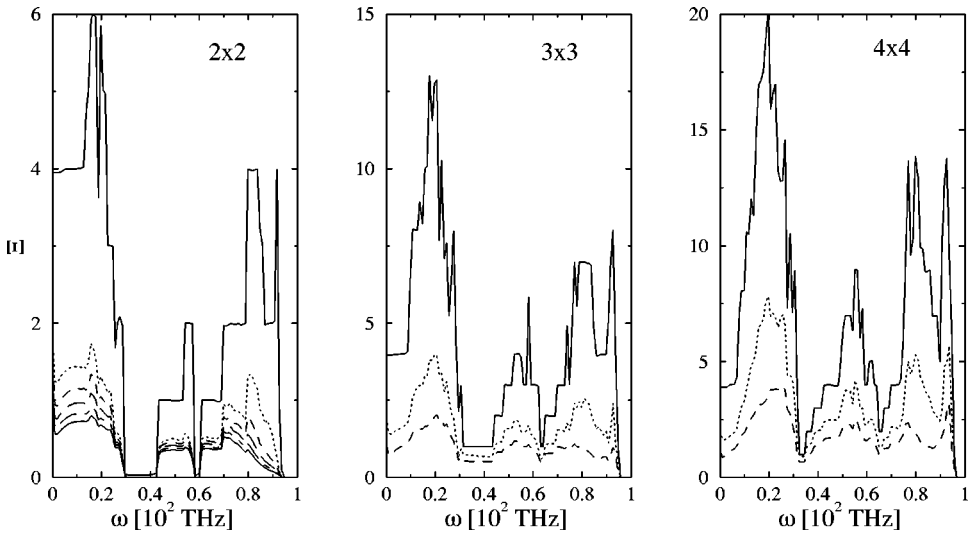

FIG. 11. SC flux transmission for Si nanowires. Left: transmission of the 2×2 wire for 0, 1, 2, 3, 4, and 5 unit cells coated. Center: transmission for the 3×3 wire with 0, 1, and 5 unit cells coated. Right: same, for the 4×4 wire.

close to four times the quantum of conductance at uncoated wires, but for wires with a thick amorphous coating the measurement will in general yield smaller values at the very low-temperature limit. Another difference pointed out earlier is the exponential decrease of conductance with length in the rough wires, as compared with the inversely proportional dependence in the long length limit for amorphous-coated wires.

We have also calculated the relaxation length λ_∞ [Eq. (40)] as a function of the Bethe lattice coverage, in Fig. 13. The abscissa corresponds to the number of Bethe lattices attached to each pair of surface atoms of the 4×4 nanowire. Since there are three spatial directions, we can attach up to six lattices to each of the pairs. We show λ_∞ as a function of the number of directions attached, for different ways of attachment. The directions in which the Bethe lattices are attached, and the number of them, are depicted schematically near the points in the graph. The calculation shows that the relaxation length is strongly dependent on the character of the bonding to the coating material. For a densely covered wire, the relaxation length becomes of the order of the wire's core diameter. On the other hand, if the surface bonds to the coating are less dense, with one dominant direction and two much weaker links in the other two directions, then the relaxation length can attain values between two and four times the diameter. When there is only partial bonding of part of the surface atoms, the relaxation length increases further. The way in which λ approaches its saturation value, λ_∞ is shown in the inset of Fig. 13. With only one link per surface atom (solid curve), it is necessary to coat a considerable length in order to attain the diffusive limit. With more interface links, the diffusive limit is reached at shorter coated lengths. It is observed that not only the number of links but also their orientation has an influence on the relaxation length.

A larger number of interface links does not necessarily imply a shorter relaxation length. A fully covered surface with three links per atom, for example, displays a larger relaxation length than a surface with only half of the surface atoms directly attached to the coating (Fig. 13). This is an-

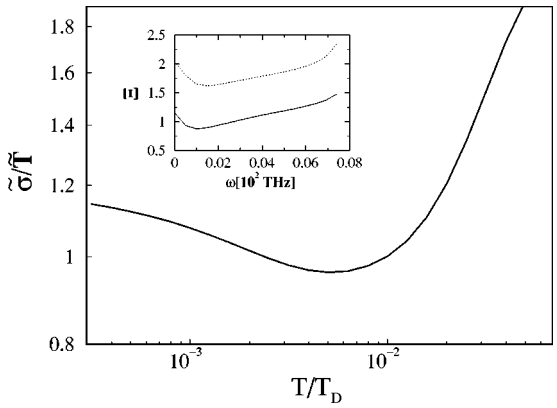

FIG. 12. Low-temperature behavior of the thermal conductance divided by temperature, for the 4×4 nanowire with 5 unit cells coated, showing a dip similar to the one studied in Ref. 11. (The ordinate axis unit is $(6/\pi)\hbar/k_B^2$.) Inset: detail of the transmission function $\Xi(\omega)$ at low frequencies, for the 4×4 wire with 1 (dotted line) and 5 (solid line) unit cells coated.

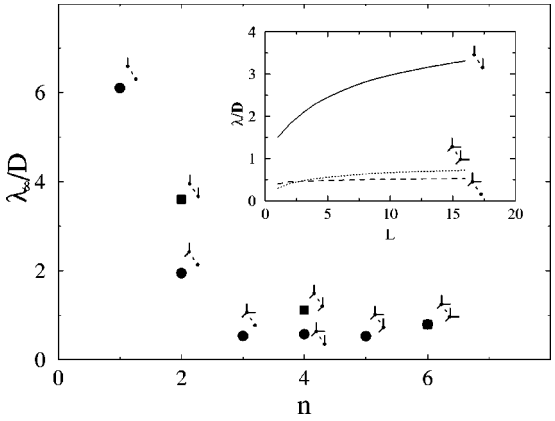

FIG. 13. Phonon relaxation length λ_∞ in 4×4 wire at frequency $\omega=16$ THz, for different ways of attachment between the coating and the wire surface atoms, in units of the wire's diameter *D*. The scheme near each data point represents the directions in which the Bethe branches are attached to each surface pair of atoms. The inset shows λ vs the coated length *L* (in unit-cell lengths), for three particular attachment configurations.

other manifestation of the phenomenon noted in Sec. III A, where we saw that a very strong interaction between wire and coating can result in longer relaxation lengths.

IV. CONCLUSIONS

We have presented a formalism to calculate the phonon transmission function of an atomically described system. With this formalism we have studied the problem of phonon transport in nanowires with part of their length coated by an amorphous material. A self-consistent approach, has been developed that uses Bethe lattices to treat the amorphous material. The efficiency of the approach, and its equivalence to a much more computationally demanding cluster calculation have been explicitly illustrated via direct comparison by an example.

We have studied two examples of amorphous-coated wires: a 1D model and silica coated Si nanowires. In the examples studied, specific physical phenomena for coated systems have arisen, given as follows.

(1) *Ballistic-diffusive transition*. We explicitly showed the evolution of the phonon transmission in the transitional regime, before $\lambda(\omega,L)$ asymptotically approaches its limiting value. In the limit of long coated length the transmission attains a $1/L$ behavior. (In contrast, for rough-boundary uncoated wires, an exponential decrease with length takes place.[11])

(2) *Low-temperature conductance*. Near $\omega=0$, the transmission is found to decrease with respect to its $\omega=0$ value, as the frequency is increased. As a result, amorphous-coated wires display a low-temperature dip in the plot of the thermal conductance divided by temperature, having certain similarities with the dip reported for rough uncoated wires.[11]

(3) *Coating-wire interface structure effects*. A phenomenon is found, which is specific of coated wires: as the interatomic bonds between wire and coating atoms are made stronger, starting from zero, the transmission of a long coated wire [or equivalently, $\lambda(L,\omega)$] decreases, but only up to a certain limit; once the bond strength reaches a certain threshold, the transmission *increases* again as the bond is made stronger. When the bond strength tends to infinity the relaxation length asymptotically saturates to a finite value. An analogous behavior was found to take place as a function of the number of interface links. The structure of the interface was shown to have an important effect on the relaxation length.

It is hoped that the method and results presented here will help to estimate further atomistic research in the field of phonon transmission through nanowires, as well as experimental research on amorphous-coated nanowires.

ACKNOWLEDGMENTS

We acknowledge Toshishige Yamada, Fuensanta Aroca, and Jawad Snoussi for valuable comments on the manuscript, and also A. Balandin and P. Schelling for useful discussions. This work was supported under NASA contract.

APPENDIX: THE ROLE OF ANHARMONICITY

In one dimension, there is no three-phonon anharmonic scattering, since it is not possible to have a process in which all three phonons belong to the same polarization branch.[35] Therefore, anharmonicity is not an issue in the first example, given in Sec. III A.

The role of anharmonicity in the thermal conductivity of Si nanowires has been studied in Ref. 41. For the wires studied in Sec. III B, its influence is negligible. An estimation can be made using the Mathiessen rule. The total relaxation length, expressed in terms of the boundary and anharmonic relaxation lengths, is

$$\lambda = 1/(\lambda_b^{-1} + \lambda_a^{-1}). \tag{A1}$$

Now, $\lambda_b \sim D$, where D is the system's thickness (around 2 nm, for the wires considered here). Also, $\lambda_a \sim c/[1.73 \times 10^{-19}(s/K)T\omega^2 e^{-137.3K/T}]$, where c is the Si speed of sound.[40] The role of anharmonicity is largest for the highest frequencies. But even for the highest frequency available in Si, ~ 95 THz, the anharmonic relaxation length at room temperature is still $\lambda_a \sim 20$ nm. This, in the case of the nanowires of Sec. III B, using Eq. (A1) and the estimate just given for λ_b, affects the transmission by less than 10%. (Lower frequencies are much less affected.) The influence on the thermal conductivity is much smaller than this, since high modes contribute significantly less than the lower-energy modes. Experimentally it has been observed that even for nanowires 37 nm thick, the effect of anharmonicity on the thermal conductivity is minimal compared to that of boundary scattering, up to 300 K. This is evident from the fact that the thermal conductivity stays constant with T near room temperature, rather than decrease (see Refs. 40 and 41).

[1] Yi Cui, Lincoln J. Lauhon, Mark S. Gudiksen, Jianfang Wang, and Charles M. Lieber, Appl. Phys. Lett. **78**, 2214 (2001).

[2] K. Schwab, E.A. Henriksen, J.M. Worlock, and M.L. Roukes, Nature (London) **404**, 974 (2000).

[3] W. Fon, K.C. Schwab, J.M. Worlock, and M.L. Roukes, Phys. Rev. B **66**, 045302 (2002).

[4] P. Kim, L. Shi, A. Majumdar, and P.L. McEuen, Phys. Rev. Lett. **87**, 215502 (2001).

[5] J. Zou and A. Balandin, J. Appl. Phys. **89**, 2932 (2001); A. Balandin and K.L. Wang, Phys. Rev. B **58**, 1544 (1998).

[6] S.G. Volz and G. Chen, Appl. Phys. Lett. **75**, 2056 (1999).

[7] P.K. Schelling, S.R. Phillpot, P. Keblinski, Phys. Rev. B **65**, 144306 (2002).

[8] A. Kambili, G. Fagas, V.I. Fal'ko, and C.J. Lambert, Phys. Rev. B **60**, 15 593 (1999).

[9] A. Ozpineci and S. Ciraci, Phys. Rev. B **63**, 125415 (2001); A. Buldum, S. Ciraci, and C.Y. Fong, J. Phys.: Condens. Matter **12**, 3349 (2000); S. Ciraci, A. Buldum, and I.P. Batra, *ibid.* **13**, R537

(2001).
[10] L.G.C. Rego and G. Kirczenow, Phys. Rev. Lett. **81**, 232 (1998); A. Greiner, L. Regglani, and T. Kuhn, *ibid.* **81**, 5037 (1998).
[11] D.H. Santamore and M.C. Cross, Phys. Rev. B **63**, 184306 (2001); *ibid.* **66**, 144302 (2002); Phys. Rev. Lett. **87**, 115502 (2001).
[12] D.E. Angelescu, M.C. Cross, and M.L. Roukes, Superlattices Microstruct. **23**, 673 (1998).
[13] M.P. Blencowe, Phys. Rev. B **59**, 4992 (1999).
[14] K.R. Patton and M.R. Geller, Phys. Rev. B **64**, 155320 (2001).
[15] D.M. Leitner and P.G. Wolynes, Phys. Rev. E **61**, 2902 (2000).
[16] D.D.D. Ma, C.S. Lee, F.C.K. Au, S.Y. Tong, and S.T. Lee, Science **299**, 1874 (2003).
[17] Y. Imry and R. Landauer, Rev. Mod. Phys. **71**, S306 (1999).
[18] W. Jones and N. H. March, *Theoretical Solid State Physics* (Dover, New York, 1985).
[19] E. N. Economou, *Green's Functions in Quantum Physics* (Springer-Verlag, Berlin, 1983).
[20] N. Mingo, Liu Yang and Jie Han, J. Phys. Chem. B, **105**, 11 142 (2001).
[21] E.C. Goldberg, A. Martín-Rodero, R. Monreal, and F. Flores, Phys. Rev. B **39**, 5684 (1989).
[22] F. Guinea, C. Tejedor, F. Flores, and E. Louis, Phys. Rev. B **28**, 4397 (1983).
[23] P. G. Klemens, in *Solid State Physics*, edited by F. Seitz and D. Turnbull (Academic, New York, 1958), Vol. 7, p. 1.; P.G. Klemens, Proc. R. Soc. London, Ser. A **208**, 108 (1951).
[24] L. Martín Moreno and J.A. Vergés, Phys. Rev. B **42**, 7193 (1990).
[25] R.B. Laughlin and J.D. Joannopoulos, Phys. Rev. B **16**, 2942 (1977).
[26] As it is customary in Green's function cluster calculations, a small imaginary part $i\delta$ is added to the frequency to smoothen singularities. To avoid spurious effects, the imaginary part has to be smaller when the density of singularities increases near the band edges, so $\delta \propto \sqrt{2-\cos^2\tilde{\omega}}/\sqrt{2}$ was used.
[27] For $\tilde{T}\to 0$ the dimensionless conductance tends to $\tilde{\sigma}\to \Xi(0)\tilde{T}$. This means that for $\Xi(0)=1$ the conductance becomes $(k_b^2\pi^2/3h)T$, i.e., one quantum of thermal conductance. Also, for a constant transmission $\Xi(\tilde{\omega})=\Xi_0$, we have $\lim_{\tilde{T}\to\infty}\tilde{\sigma}=3\pi^2\Xi_0$.
[28] J. Callaway, Phys. Rev. **113**, 1046 (1959).
[29] M.G. Holland, Phys. Rev. **132**, 2461 (1963).
[30] M. Asen-Palmer, K. Bartkowski, E. Gmelin, M. Cardona, A.P. Zhernov, A.V. Inyushkin, A. Taldenkov, V.I. Ozhogin, K.M. Itoh, and E.E. Haller, Phys. Rev. B **56**, 9431 (1997).
[31] C.W.J. Beenakker, Rev. Mod. Phys. **69**, 731 (1997).
[32] M.J.M. de Jong, Phys. Rev. B **49**, 7778 (1994).
[33] This can be understood as the presence of the amorphous coating giving the wire a three-dimensional character and preventing localization.
[34] J. M. Ziman, in *Electrons and Phonons* (Clarendon, Oxford, 1963).
[35] W. A. Harrison, *Electronic Structure and the Properties of Solids* (Dover, New York, 1989).
[36] W. Weber, Phys. Rev. B **15**, 4789 (1977).
[37] G. Nilsson and G. Nelin, Phys. Rev. B **6**, 3777 (1972).
[38] C.-K. Loong, J. Eur. Ceram. Soc. **19**, 2241 (1999).
[39] N. Nishiguchi, Y. Ando, and M.N. Wybourne, J. Phys.: Condens. Matter **9**, 5751 (1997).
[40] N. Mingo, Phys. Rev. B **68**, 113308 (2003).
[41] D. Li, Y. Wu, P. Kim, L. Shi, P. Yang, and A. Majumdar, Appl. Phys. Lett. **83**, 2934 (2003).